Available online at www.sciencedirect.com
SCIENCE DIRECT
Journal of Solid State Chemistry 179 (2006) 1318–1322
JOURNAL OF SOLID STATE CHEMISTRY
www.elsevier.com/locate/jssc

Synthesis, structure and properties of a new Zintl phase: SrLiSb

Shalabh Gupta, Ashok K. Ganguli*

Department of Chemistry, Indian Institute of Technology Delhi, Hauz Khas, New Delhi 110016, India

Received 3 November 2005; received in revised form 17 January 2006; accepted 22 January 2006
Available online 9 March 2006

Abstract

A new ternary antimonide SrLiSb has been synthesized and characterized using single-crystal X-ray studies. It is found to crystallize in the anti-$PbCl_2$ structure type with orthorhombic cell (centrosymmetric S.G., *Pnma*; $a = 8.0408(8)$ Å, $b = 4.8145(5)$ Å, $c = 8.4517(9)$ Å) and is isostructural to its calcium analogue (CaLiSb). However, BaLiSb has been reported to crystallize in the hexagonal space group $P6_3/mmc$. As in the Ca and Ba analogues, antimony is present as isolated Sb^{3-} ions making SrLiSb electron precise and hence is expected to behave as a classical Zintl compound. The magnetic susceptibility measurements show the diamagnetic nature and the conductivity is temperature independent, both verifying the classical Zintl nature of SrLiSb.

Keywords: Antimonide; Crystal structure; Anti-$PbCl_2$ structure; Trigonal prisms; Magnetic susceptibility

1. Introduction

The area of polar intermetallic compounds has witnessed the discovery of several novel structures in the past [1–3]. These compounds, which are formed with electropositive elements (alkali and alkaline earth) and the elements on the Zintl border such as Sn and Sb, display a rich variety of structural features and novel electronic properties that require understanding of new concepts like metallic Zintl phases [4,5] and the effect of packing and non-classical bonding [6–8]. The alkaline-earth–tin and alkaline-earth–antimony systems have been of interest among researchers in this field [9,10]. The exploratory nature of the activities involved in this kind of research often comes as surprise in the form of unknown structure types and quite often leads to completion of the missing compounds in a known structural family. The novel properties often encountered for these compounds arise from their interesting electronic position between the intermetallics and the true valence compounds. Various ternary phases of the type *ABX* where *A* and *B* are either alkaline earth elements or mixed alkali and alkaline earth elements with *X* being the main group elements from group 14 and 15 have been reported. These include compounds of the type (Ca, Ba, Sr)Mg*X* (*X* = Si, Ge, Sn, Pb) [11] and CaLiSb [12], BaLiSb [13] and $(Ba/Sr)_3Li_4Sb_4$ [14]. As has been well documented in the literature cations play an important role in the formation of the anionic substructure [15,16]. Size of the cations and their polarizing power (density of charge) seems to affect the formation of different Zintl polyanions of the type E_n^{m-}. For example, Mg^{2+} ions with its small size, leads to a highly charged mono-anionic lattice (cluster or isolated), whereas larger cations and others with low charge density leads to considerable bonding. This can be observed in the *ABX* type of compounds where CaMg*X* and SrMg*X* (*X* = Si, Ge, Sn and Pb) [11] crystallize in anti-$PbCl_2$ type lattice [17] (orthorhombic system, *Pnma*) whereas the Ba analogues crystallize in the anti-PbFCl type lattice (orthorhombic, *Pnma*). Investigation of one such system involving the Ca_2Tt–Mg_2Tt systems (Tetrel (*Tt*) = Sn, Pb) led to the discovery of new structural relationships within $Ca_{2-x}Mg_xTt$ system [18]. In this ternary system, the Co_2Si structure (orthorhombic, *Pnma*) [19] exists for $0 \leqslant x \leqslant 1$ beyond which Mg_2Sn phase with the anti-fluorite structure (cubic, *Fm*3*m*) is present. No Mg rich phase ($x > 1$) was observed to crystallize in Co_2Si structure type, suggesting that an important role is played by the cation size in stabilizing the structure. Unlike M_2X compounds (*M* = Ca, Sr, Ba; *X* = Si, Ge, Sn, Pb), which crystallize

*Corresponding author. Fax: +91 11 26854715.
E-mail address: ashok@chemistry.iitd.ernet.in (A.K. Ganguli).

0022-4596/$ - see front matter © 2006 Elsevier Inc. All rights reserved.
doi:10.1016/j.jssc.2006.01.059

in the orthorhombic anti-$PbCl_2$ type structure (space group *Pnma*) [20], the M_2Sb compounds (M = Ca, Sr, Ba) [21–23] crystallize in the tetragonal $I4/mmm$ space group emphasizing the role played by the electronic charge and electronegativity of anions on the structure stability. It may be noted that the Co_2Si-type structure is assigned within a broader $PbCl_2$ structure type. Not many isotypic antimony analogues, *AB*Sb (*A* and *B* being alkali or alkaline earth elements) are known in literature. CaLiSb seems to be the only example known so far to crystallize in the ordered anti-$PbCl_2$ type. Another example known for the equiatomic mixed alkali–alkaline earth antimonide is RbCaSb [24]. This compound however crystallizes in a tetragonal space group $P4/nmm$ with different lattice parameters. The equiatomic barium lithium antimonide (BaLiSb) crystallizes in the centrosymmetric hexagonal space group $P6_3/mmc$ though with similar lattice parameters as CaLiSb. BaLiSb is isostructural with KZnSb [25] and NaBeSb [26] but with interchanged positions of monovalent and divalent cation. Two more related examples of antimonides, though not equiatomic have been reported. $Sr_3Li_4Sb_4$ [14] and $Ba_3Li_4Sb_4$ [14] crystallize in *Immm* space group ($a = 15.84$; $b = 4.88$; $c = 7.50$ Å and $a = 17.18$; $b = 4.91$; $c = 7.70$ Å, respectively), which contains two different anionic moieties, isolated Sb^{3-} and Sb_2^{4-} ions. The calcium analogue has not been reported so far. Unlike the above compounds, CaLiSb and BaLiSb compounds contain only isolated Sb^{-3} anions as has also been found in the title compound.

2. Experimental section

2.1. Syntheses

Nearly monophasic samples of SrLiSb were obtained from the direct fusion of pure elements. Lithium (Aesar 99.99%), strontium (Aesar 99.8%) and antimony (Johnson Mathey 99.9%), were weighed in stoichiometric amount, loaded in Ta tubes, welded under helium atmosphere and then jacketed within fused silica containers that were well flamed under high vacuum prior to sealing. All the metals were stored and handled in a helium filled glove box. The nominal composition of the loaded mixture from which the crystal of SrLiSb was obtained was $SrLiSb_3$. The reaction mixture was heated to 850 °C at the rate of 300 °C/h and soaked for 2 h, followed by annealing at 750 °C for 96 h and subsequently cooled at the rate of 3 °C per hour up to 400 °C. Thereafter the mixture was allowed to cool normally. SrLiSb sample with ~85% phase purity could be obtained under the above-mentioned conditions in Ta container when the components were loaded in stoichiometric amounts, the other phase being Ta_5Sb_4. Interestingly greater than 95% purity was obtained under similar conditions when Nb containers were used.

2.2. Powder X-ray diffraction

The powder diffraction patterns of polycrystalline SrLiSb was obtained from the Huber 670 Guinier camera using Cu$K\alpha$1 radiation and was used for determining the phase purity of crystalline SrLiSb. Sample was mounted between two Mylar sheets using a block and ring assembly inside the nitrogen filled box. The homogeneity of the title phase loaded on stoichiometry to obtain the pure compound was established by matching the observed powder X-ray diffraction pattern with the powder pattern generated using the lattice parameters, space group, and the atomic positions from the single-crystal studies.

2.3. Single-crystal structure determination

Several irregular crystals from the product mixture were selected and saved in Lindemann glass capillaries in a glovebox designed for this purpose. Crystals were examined for singularity and the data set was collected on the best crystal available, on a Bruker APEX CCD diffractometer with the aid of monochromated Mo$K\alpha$ radiation. The data collection took place over a Θ range of ~3.50–28.25°. The detector was placed at a distance of 5.995 cm from the crystal. Three sets of 606 frames were collected with a scan width of 0.3° in ω and an exposure of 10 s per frame. The frames were integrated with the SAINT program in the SMART software package [27]. Data were corrected for absorption effects using the multi-scan techniques in SADABS [27]. The structure was solved by direct methods and refined by full matrix least-squares on F_o^2 with the SHELXTL Version 6.1 program package [28].

The systematic extinctions were consistent with space groups $Pna2_1$ (No. 33) and *Pnma* (No. 62). The $\langle E^2-1 \rangle$ values being closer to that expected for non-centrosymmetric space group along with the better combined figure of merits lead us to select the former space group for the initial solution. The structure could be refined well in this space group. However, the choice of the selected non-centrosymmetric space group was in doubt during the absolute structure parameter refinement, which leads to the ambiguous Flack parameter of 0.5. This led us to examine the centrosymmetric *Pnma* space group and was subsequently selected to obtain the correct solution. It may be noted that a related compound CaLiSb also crystallizes in the *Pnma* space group. The structure solution was carried out using direct methods. Seven systematic absence violations albeit of very low intensities were observed in both the space groups. The positional coordinates for Sb and Sr as suggested by the initial solution could be refined satisfactorily. The position for Li was subsequently ascribed to the residual of ~5 e/Å^3 in the difference Fourier map. Prior to the Li assignment, anisotropic refinement for the strontium and antimony atoms was carried out which led to well behaved ellipsoids for the two atoms. Anisotropic refinement of Li resulted in high uncertainties/U_{ij} ratio. The final refinement with 17 variables

converged at $R_1 = 2.14\%$ for observed data ($I > 2\sigma(I)$) and $wR_2 = 5.21\%$ for all data. The refinement details along with the data collection parameters are listed in Table 1. The positional coordinates for the atoms and the anisotropic displacement parameters for Sb and Sr atoms are listed in Tables 2 and 3, respectively.

Table 1
Crystal data and structure refinement for SrLiSb

Empirical formula	SrLiSb
Formula weight	216.31
Temperature	298(2) K
Wavelength	0.71073 Å
Crystal system	Orthorhombic
Space group	*Pnma*
Unit cell dimensions	$a = 8.0436(8)$ Å, $\alpha = 90^\circ$
	$b = 4.8163(5)$ Å, $\beta = 90^\circ$
	$c = 8.4547(9)$ Å, $\gamma = 90^\circ$
Volume, Z	327.54(6) Å^3, 4
Density (calculated)	4.387 Mg/m^3
Absorption coefficient	24.208 mm^{-1}
$F(000)$	368
Crystal size	$0.07 \times 0.07 \times 0.05$ mm^3
Theta range for data collection	3.50–28.25°
Index ranges	$-10 \leqslant h \leqslant 10$, $-6 \leqslant k \leqslant 6$, $-11 \leqslant l \leqslant 11$
Reflections collected	2554
Independent reflections	444 [R(int) = 0.0345]
Completeness to $\theta = 28.25^\circ$	97.4%
Refinement method	Full-matrix least-squares on F^2
Data/restraints/parameters	444/0/17
Goodness-of-fit on F^2	1.164
Final R indices [$I > 2\sigma(I)$]	$R_1 = 0.0202$, $wR_2 = 0.0490$
R indices (all data)	$R_1 = 0.0206$, $wR_2 = 0.0493$
Extinction coefficient	0.091(3)
Largest diff. peak and hole	0.741 and −1.715 e Å^{-3}

$R_1 = \sum(|F_o - F_c|)/\sum(|F_o|)$. $wR_2 = [\sum(F_o^2 - F_c^2)/\sum wF_o^4]^{1/2}$. GOF $= [\sum w(F_o^2 - F_c^2)/(n-p)]^{1/2}$ where n is the number of reflections and p is the number of parameters refined.

Table 2
Atomic coordinates ($\times 10^4$) and equivalent isotropic displacement parameters (Å$^2 \times 10^3$) for SrLiSb

	x	y	z	U(eq)
Sb(1)	2752(1)	2500	5927(1)	9(1)
Sr(2)	34(1)	2500	2909(1)	11(1)
Li(1)	3390(12)	−2500	4243(10)	19(2)

U(eq) is defined as one third of the trace of the orthogonalized U_{ij} tensor.

Table 3
Anisotropic displacement parameters (Å$^2 \times 10^3$) for SrLiSb

	U_{11}	U_{22}	U_{33}	U_{23}	U_{13}	U_{12}
Sb(1)	12(1)	6(1)	8(1)	0	0(1)	0
Sr(2)	13(1)	10(1)	11(1)	0	1(1)	0

The anisotropic displacement factor exponent takes the form: $-2p2[h2a*2U_{11} + \cdots + 2hka*b*U_{12}]$.

2.4. Physical property measurements

Electrical resistivity of nearly single-phase (>95%) samples of SrLiSb was measured at 34 MHz by the electrodeless "Q" method over a range of 110–294 K [29]. The powdered sample that had been sieved to a grain size between 150 and 250 μm was dispersed in chromatographic grade Al_2O_3. Magnetic susceptibility of this sample was obtained at a field of 3 T over a range of 6–300 K with the aid of a Quantum design (MPMS) SQUID magnetometer. The sample was accurately weighed and held between two fused silica rods within a tightly fitting outer silica tube and sealed under helium [30]. The raw data were corrected for the susceptibility of the container and the diamagnetic contributions of the ion cores [31].

3. Result and discussion

SrLiSb, a new ternary antimonide, crystallizing in the ordered anti-$PbCl_2$ type structure with three distinct crystallographic sites, has been synthesized for the first time. The crystal structure is best described as consisting of tricapped trigonal prisms (TCTP) of cations around the isolated Sb^{3-} ions as shown in Fig. 1. The coordination around antimony (dawn at 3.5 Å) shown in Fig. 2 indicate that there are no Sb–Sb contacts that is, they exist as isolated Sb^{3-} anions. At this point it is essential to bring out the subtle difference between the anti-$PbCl_2$ structure type and the Co_2Si structure type, closely related and often confused with the former. A detailed investigation of several ternary metal-rich phosphides [32] and others crystallizing in these related structure types has lead to a general criterion for the stability of the two structures as discussed below. Though this formulation eludes a clear

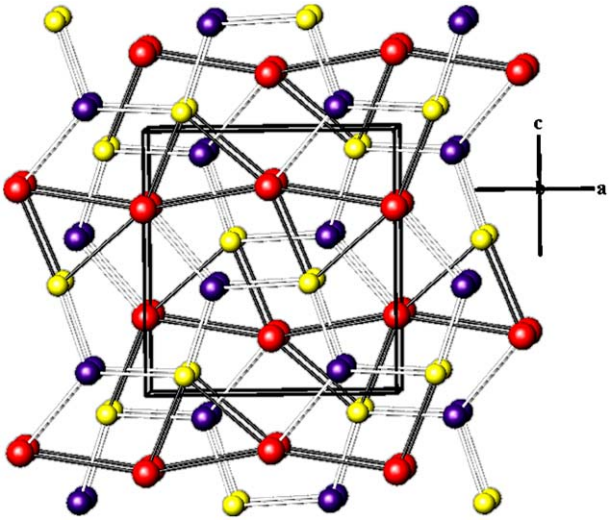

Fig. 1. An ~[010] representation of the structure of SrLiSb. Indigo represent antimony atoms surrounded by red and the yellow spheres representing strontium and lithium atoms respectively forming the corners of trigonal prisms. The trigonal prisms are linked through Sr forming the zig-zag chains of trigonal prismatic columns.

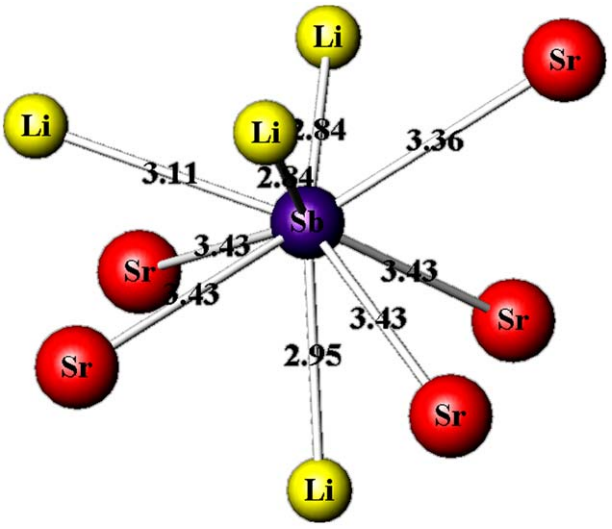

Fig. 2. Coordination around antimony along with the interatomic distances (Å).

line of distinction between the two, the anti-$PbCl_2$ occurs with a/b ratio lying between 1.50 and 1.90 whereas the stability region for Co_2Si type structure is $1.25 \leqslant a/b \leqslant 1.40$ [33]. In this regard SrLiSb with a/b ratio of 1.67 can well be described as having an anti-$PbCl_2$ structure type. One look at the coordination numbers of Sb clearly indicates 6 prismatic (2 Ca and 4 Sr) and 3 capping atom, making an ideal TCTP environment with 9 coordinated Sb (6 + 3). Co_2Si structure type with a lower a/b ratio leads to squeezing of puckered sheets thereby increasing the coordination of the central atom to 10 (6 + 4). The trigonal prisms are confacial along the shortest axis (b-axis), the separation being 4.8163(8) Å. Edge-shared zig-zag chains of the trigonal prisms run along the 'a' direction. The chains are formed by the edge sharing of the four vertices, the other two remaining free. The neighboring chains are aligned along the c-axis. The trigonal prisms of one chain are capped on the two faces by Li atoms of the other chain, which occupy the unshared vertices of the prisms and by the Sr atom on the third face. The capping Li atoms are at 2.946(7) Å and 3.108(8) Å and Sr at 3.358(5) Å from the Sb atom. The Sr–Sr side edges link together in zig-zag fashion along the 'a' axis to form infinite chain. The unique position occupied by the smaller Li atoms at the unshared vertex of the trigonal prisms result in the low-dimensional behavior (zig-zag chains along 'a') which also allows a stronger Li–Sb bonding. This effect is well reflected in $Ca_{2-x}Mg_xSn$ system where on substitution, the smaller Mg atoms preferentially occupy the vertex positions [18]. A trigonal prism motif exhibiting this site preference is also reported in $Ca_{6.2}Mg_{3.8}Sn_7$ [16]. This compound affords a good example of the effect of mixed cations on stabilization of novel anionic substructure. This structure is built of trigonal prisms of Ca and Mg atoms centered by Sn. Two different chains of trigonal prisms run along the 'a' axis and alternate along the 'b' axis. Chains of trigonal prisms centered by Sn at $z = 0, 1$ is composed of a single type of prism built of Ca and Mg sharing two of its Ca–Ca side edges to generate an infinite zigzag chains. These trigonal prisms are centered by Sn atoms which remains isolated with d(Sn–Sn) > 4.0 Å. In the alternating chain, a more impressive arrangement of four trigonal prisms sharing Ca–Ca edges to generate a slightly distorted cube of Ca atoms centered by Sn is observed. SrLiSb adopts a relatively simpler structure consisting only of the former where the trigonal prisms are centered by isolated Sb^{3-} with no d(Sb–Sb) < 4.8 Å. It has been observed that the structure adopted by $Ca_{6.2}Mg_{3.8}Sn_7$ ceases to exist in the absence of Mg suggesting the role played by Mg in achieving increased coordination number for Sn. The coordination environment of Mg, with half the atoms being contributed by the two adjacent chains each, suggests that Mg is essential to the interchain bonding. The same seems true for the present system where the shorter Li–Sb (3.108(8) Å) interchain bonding could be expected to be more effective in glueing the chains together than the Sr–Li (3.3580(5) Å) interchain bonds. It may be noted that Ca_2Sb and the isotypic Sr_2Sb prefers a more symmetric tetragonal system consisting of distorted tetragonal antiprisms. As has been observed in Ca_2Sn, the off-centering of Sb in the trigonal prisms is quite considerable, with Sb atoms moving closer to the Li atoms. On comparing the radii and elctronegativites of Sn, Sb, Sr and Ca, more covalent overlap could be expected for Sr–Sb pair compared to Ca–Sn pair. This is manifested in the smaller Sr–Sb distance compared to Ca–Sn inspite of larger Sr radii (2.0 Å) compared to Ca (1.80 Å) [34], those of Sn and Sb being very similar (1.45 Å) [32]. However, compared to SrLiSb the distances of prismatic cations from the central Sb in CaLiSb is in accord with the smaller Ca radii.

Polycrystalline sample of SrLiSb (>95% phase purity) shows non-metallic behavior with negligible temperature dependence. The molar susceptibility for this compound exhibit a weak and essentially temperature independent

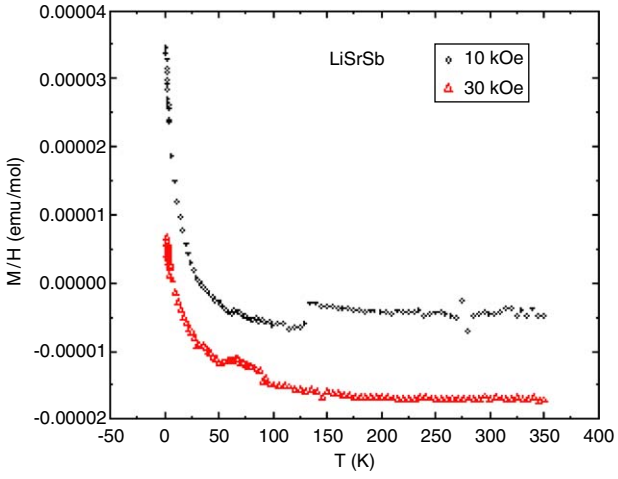

Fig. 3. Variation of molar magnetic susceptibility with temperature for SrLiSb.

diamagnetism above about 100 K as shown in Fig. 3. The weak diamagnetic signal along with non-metallic behavior suggests the sample to be a classical Zintl compound.

Acknowledgments

The authors thank Department of Science and Technology, Government of India and IIT Delhi for the funding of the Bruker SMART APEX X-ray diffractometer. The authors also thank Professor J.D. Corbett, Iowa State University, for supporting (from his NSF Grant DMR-0129785) the visit of A.K.G. and S.G. to ISU and Ames Laboratory of the US Department of Energy (DOE) where part of this research was carried out.

References

[1] J.D. Corbett, Angew. Chem. Int. Ed. 39 (2000) 670.
[2] J.D. Corbett, in: S. Kauzlarich (Ed.), Chemistry, Structure and Bonding of Zintl Phases and Ions, VCH, New York, 1996 (Chapter 3).
[3] H. Schaefer, Ann. Rev. Mater. Sci. 15 (1985) 1.
[4] R. Nesper, Prog. Solid State Chem. 20 (1990) 1.
[5] R. Nesper, Angew Chem., Int. Ed. Eng. 30 (1991) 789.
[6] J.D. Corbett, Chem. Rev. 85 (1985) 383.
[7] S.C. Sevov, J.D. Corbett, Inorg. Chem. 30 (1991) 4875.
[8] Z.-C. Dong, J.D. Corbett, J. Am. Chem. Soc. 116 (1994) 3429.
[9] A.K. Ganguli, A.M. Guloy, E.A. Leon-Escamilla, J.D. Corbett, Inorg. Chem. 32 (1993) 4349.
[10] G. Derrien, M. Tillard-Charbonnel, A. Manteghetti, L. Monconduit, C. Belin, J. Solid State Chem. 164 (2002) 169.
[11] B. Eisenmann, H. Schaefer, A. Weiss, Z. Anorg. Allgem. Chem. 391 (1972) 241.
[12] B. Eisenmann, O. Liebrich, H. Schaefer, A. Weiss, Z. Naturforsch. Teil B 24 (1969) 1344.
[13] L. Monconduit, C. Belin, Acta Crystallogr. E: Struct. Rep. Online E 57 (2001) E57 i17.
[14] O. Liebrich, H. Schaefer, A. Weiss, Z. Naturforsch. Teil B 25 (1970) 650.
[15] A. Currao, J. Curda, R. Nesper, Z. Anorg. Allg. Chem. 622 (1996) 85.
[16] A.K. Ganguli, J.D. Corbett, M. Köckerling, J. Am. Chem. Soc. 120 (1998) 1223.
[17] K. Sahl, Beitr: Mineral. Petrogr. 9 (1963) 111.
[18] A. Ganguli, A.M. Guloy, J.D. Corbett, J. Solid State Chem. 152 (2000) 474.
[19] S. Geller, V.M. Wolontis, Acta Crystallogr. 8 (1955) 83.
[20] G. Bruzzone, E. Franceschi, J. Less-Common Met. 57 (1978) 201.
[21] B. Eisenmann, H. Schaefer, Z. Naturforsch. Teil B 29 (1974) 13.
[22] M. Martinez-Ripoll, A. Haase, G. Brauer, Acta Crystallogr. B 29 (1973) 1715.
[23] B. Eisenmann, K. Deller, Z. Naturforsch. Teil B 30B (1975) 66.
[24] R.H. Cardaso Gil, N. Caroca-Canales, W. Hoenle, H.G. Von Schnering, Z. Kristallogr. 213 (1998) 455.
[25] G. Savelsberg, H. Schaefer, Z. Naturforsch. Teil B 33B (1978) 370.
[26] C. Tiburtius, H.U. Schuster, Z. Naturforsch. Teil B 32B (1977) 1133.
[27] SMART, Bruker AXS, Inc., Madison, WI, 1996.
[28] SHELXTL, Bruker AXS, Inc., Madison, WI, 2000.
[29] J.T. Zhao, J.D. Corbett, Inorg. Chem. 34 (1995) 378.
[30] S.C. Sevov, J.D. Corbett, Inorg. Chem. 31 (1992) 1895.
[31] P. Selwood, Magnetochemistry, Second ed., InterScience Publishers, New York, 1956, p. 78.
[32] G.J. Miller, J. Cheng, Inorg. Chem. 34 (1995) 2962.
[33] W. Jeitschko, Acta Crystallogr. B 24 (1968) 930.
[34] R.D. Shannon, Acta Crystallogr. 32A (1976) 751.